energies

MDPI

*Article*

# Grid Connection of a Squirrel-Cage Induction Generator Excited by a Partial Power Converter

**Dominik A. Górski [1,*], Grzegorz Dziechciaruk [1] and Grzegorz Iwański [1,2,*]**

[1] Institute of Control and Industrial Electronics, Warsaw University of Technology, 00-662 Warsaw, Poland; grzegorz.dziechciaruk@pw.edu.pl
[2] Automatic Control and Computer Science, Faculty of Electrical Engineering, Kielce University of Technology, 25-314 Kielce, Poland
* Correspondence: dominik.gorski@pw.edu.pl (D.A.G.); grzegorz.iwanski@pw.edu.pl (G.I.)

**Abstract:** This article concerns the connection process of a squirrel-cage induction generator to the grid/microgrid. Typically, the generator is unexcited, and its connection to the grid is made directly via a switch. This connection causes a high inrush current and grid voltage drop, which local consumers notice. This article proposes a robust power system consisting of the squirrel-cage induction generator, a power electronic converter, and a capacitor bank, all connected in parallel. The proposed configuration and a dedicated control system eliminate the inrush current and compensate for the generator's reactive power during grid-tied operation. The converter controls the generator voltage build-up to adjust the generator voltage to the grid voltage (controlled excitation) and connects the generator to the grid, minimising distortions. Moreover, the system is robust because the failure of the converter does not stop the power generation, unlike a system with a back-to-back converter, where the converter links the generator and the grid. Furthermore, the parallel-connected converter has a significantly reduced power rating because it is only rated for a part of the reactive generator power. The rest of the reactive generator power is delivered by the fixed capacitor bank. The article presents the system configuration, the control method, and laboratory results confirming the system's effectiveness in maintaining high-quality grid voltage during generator-to-grid connection and high-quality power supplied to the grid.

**Keywords:** squirrel-cage induction generator; power electronic converter; partial power converter; grid connection; synchronisation



Academic Editor: Dinko Vukadinović

Received: 8 December 2024
Revised: 6 January 2025
Accepted: 11 January 2025
Published: 16 January 2025

**Citation:** Górski, D.A.; Dziechciaruk, G.; Iwański, G. Grid Connection of a Squirrel-Cage Induction Generator Excited by a Partial Power Converter. *Energies* **2025**, *18*, 368. https://doi.org/10.3390/en18020368



## 1. Introduction

Squirrel-cage induction generators are widely used with small wind- and hydro-turbines as well as biogas combustion engines. The simplicity of connecting induction generators to the grid is the main reason for their use in such systems. They are frequently used in power systems without rotational speed control or in systems with coarse speed regulation. Therefore, the power system is simple and robust. The grid connection of the induction generator can be performed at any generator speed, but it usually takes place near the synchronous speed [1–5]. Nevertheless, the grid operation of the induction generator requires super-synchronous speed, so the prime mover has to provide it in normal operation mode. In such simple systems, two main methods of generator connection to the grid are used:

1. Direct connection of the unexcited generator to the grid;
2. Connection using a thyristor soft-starter [6–9].

The direct connection methods cause a high inrush current and a voltage dip in the local grid [4]. Soft-starters limit the inrush current, but introduce harmonics during the connection process and remain unused after the connection [6].

The most comprehensive solution adopts two integrated AC/DC converters with a common DC-link (back-to-back converter) as an interface between the generator and the grid, as depicted in Figure 1a. Then, the grid connection does not induce any inrush current, and generator operation is possible at either super-synchronous or sub-synchronous speed. However, such a system requires two full-scale power electronic converters [10–12], and the failure of the converter stops the power generation.

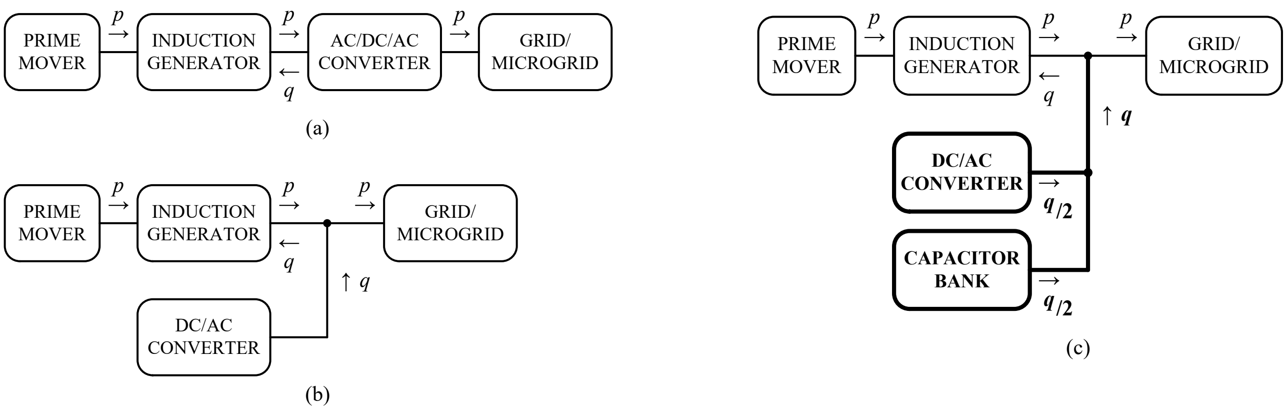


**Figure 1.** The power system configurations equipped with a squirrel-cage induction generator and a power electronic converter: (**a**) system with a back-to-back converter; (**b**) system with a parallel connected full reactive power converter; (**c**) system with a parallel connected partial reactive power converter.

The system shown in Figure 1b uses an AC/DC converter connected in parallel to the generator. The main advantage of this system is the reduced size of the converter because it is only rated for the generator's reactive power. As mentioned before, the generator's connection to the grid can be achieved by directly connecting the rotating generator to the grid, which induces an inrush current and voltage drop in the local grid [1,4]. However, a more modern approach is the asynchronous connection process, involving two steps [13]. The first step is a controlled excitation process of the generator provided by the converter. This process equalises the amplitudes of the generator voltage with the grid voltage. The second step is detecting the proper moment of the generator connection by the control system. The connection of the generator is achieved when the voltage vectors overlap despite the different angular frequencies of the vectors (only their angles match one another) [13]. This approach can significantly reduce inrush currents and disturbances in the grid at the moment of the generator connection. A more sophisticated generator connection is possible if the converter, besides giving excitation, loads the generator. Then, grid and generator voltage synchronisation is possible, and the generator connection is activated at synchronised voltages. This approach eliminates inrush current when connecting the generator to the grid [14].

This article proposes a new system configuration, further reducing the converter rated power. The goal is achieved by adding the capacitor bank (CB) in parallel to the converter and generator. A general scheme of the system is presented in Figure 1c. In this system configuration, the capacitor bank provides part of the reactive power demand and the converter delivers the rest. The system has several significant advantages. Firstly, the system can obtain the synchronised connection of the generator to the grid, which eliminates inrush current. Secondly, it is still simple and robust. The converter only provides some of the generator power, so the failure of the converter does not stop the operation of the generator. The converter can be disconnected from the system and the generator can continue its operation, but with a worse power factor. In comparison, the system shown in Figure 1a has a two-stage power conversion. It must transfer the full power produced by the generator, so power losses in converters are related to reactive and active generator power. In the proposed system, the generator is directly connected to the grid and the converter losses are only related to the reactive power. Nevertheless, both systems can continuously compensate for the reactive power variation resulting from the generator operation. A comparison of the SCIG connection systems is summarised in Table 1.

**Table 1.** Comparison of the SCIG connection systems.

| Connection System Type | Direct Connection | Soft-Start | Back-to-Back Converter | Parallel Converter | Parallel Partial Power Converter |
|---|---|---|---|---|---|
| Power electronic component of the system | No extra elements | Soft-start circuit | Two-stage converter (AC/DC and DC/AC) | Single-stage converter (AC/DC) | Single-stage converter (AC/DC) |
| Converter power rating value | - | - | Apparent power of the generator (the highest value) | Reactive generator power (medium value) | Part of reactive generator power (low value) |
| Capacitor bank | Required | Required | Not required | Not required | Partially required |
| Inrush grid current at the generator connection | High | Limited | None | None | None |
| Reactive power regulation | No, requires additional system | No, requires additional system | Yes | Yes | Yes |
| Possibility of operation with broken converter | Yes | Yes | No | Yes, with bad PF | Yes, with moderate PF |
| Prime mover operation speed range | Fixed speed, above synchronous | Fixed speed, above synchronous | Full range | Fixed speed, above synchronous | Fixed speed, above synchronous |

The control system for the proposed topology has been designed to include the option of synchronous or asynchronous connection. A general description of these connection methods and the details of the control system are presented in the first part of the article. For the proposed system, the controlled connection process might be impossible if the capacitance of the capacitor bank is wrongly selected. The capacitor bank may cause the uncontrolled excitation of the generator at the first stage of the generator connection process when the prime mover spins the generator. Therefore, later in this paper, an analysis of the selection of capacitor bank capacitance is presented. The analysis considers the characteristics of the induction generator and prime mover. Then, the laboratory validation of the generator's connection to the grid using the proposed system topology and control method is presented. Finally, the conclusions are given.

In summary, the authors of this paper propose a new system configuration/topology, further reducing the rated converter power. For this configuration, the methodology for capacitor bank selection is presented. The control system is redesigned to integrate two previously published control methods [13,14]. The new power system configuration is experimentally validated. Moreover, the experimental results of the proposed system are compared to those of the two other system configurations and connection methods.

## 2. Proposed Methods of Grid Connection of Induction Generator

The proposed control system can connect the generator to the grid using the synchronous or asynchronous method. These control methods require slightly different hardware configurations, which can be adjusted to meet specific needs. The choice of connection method compromises system simplicity and the reduction of disturbances in the grid during the connection process. The synchronised connection method almost entirely eliminates any disturbances in the grid caused by the generator connection process, but requires a controllable load. In comparison, the asynchronous connection method does not require generator loading, even though it significantly reduces disturbances during generator connection. The system configurations needed for these methods are outlined in Figure 2a,b. The system with the squirrel-cage induction generator in Figure 2a utilises, apart from the capacitor bank (CB) and the power electronic converter (PEC), a controlled load (CL) for loading the generator. This system configuration is used to synchronise the generator's connection to the grid. Figure 2c describes the general algorithm of the connection process for both methods, which has been implemented in the proposed control system. The figure only introduces the main idea of the control algorithm. Further details of the algorithm and control process are described in the section titled "Control System".

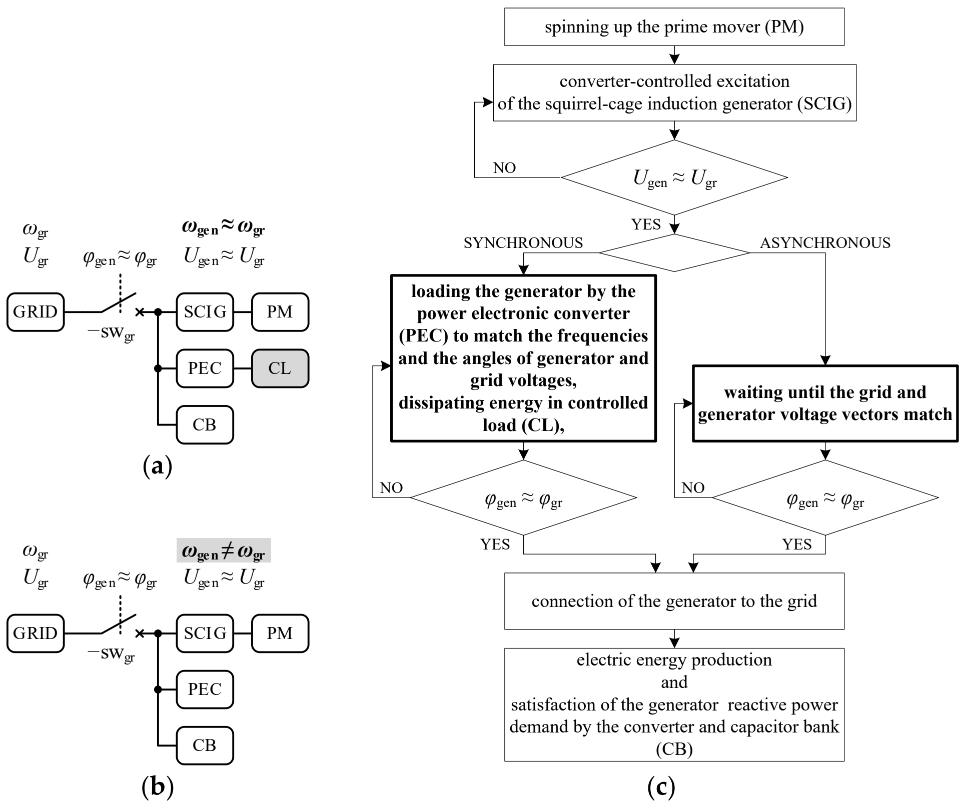


**Figure 2.** Universal algorithm for the grid connection of an excited squirrel-cage induction generator (SCIG): (**a**) system block schematic for the method of synchronising the generator voltage with the grid voltage by loading the induction generator; (**b**) system block diagram for the asynchronous connection method, where the generator and grid voltage vectors match, but the frequencies are different; (**c**) general algorithm of the generator-to-grid connection.

The proposed generator connection process always begins with the induction generator being spun by the prime mover. The generator should obtain a super-synchronous speed, like in typical power plant system. When the speed of the generator has settled down, the excitation of the induction generator begins. The energised converter controls the excitation process, where the amplitude of the generator voltage is regulated. The process is finished when the RMS values of the generator $U_{gen}$ and grid $U_{gr}$ voltage are equal with an assumed tolerance. Then, the control depends on the selected method. In the synchronised connection method, the controlled load, connected to the converter DC-link, is used to load the generator via the converter. The converter reduces the generator speed by loading the generator in a controllable manner. Therefore, the control system can match the frequencies and phases of the generator and the grid voltages. When the phases of the voltages match one another, the grid switch closes ($-sw_{gr}$) and the connection of the generator to the grid is established. From this moment, the generator delivers energy to the grid while the power electronic converter delivers a reactive current depending on the induction generator's power demand.

The configuration of the power system can be simplified even more. If the controlled load is removed, as presented in Figure 2b, only the asynchronous connection method can be used. Asynchronous connection is possible because the generator connection is made when the voltage vectors of the generator and grid overlap periodically without affecting the generator's frequency (related to the rotational speed). In this case, the generator speed should be as close to the synchronous speed as possible. In comparison to the previous connection method, the frequency of the generator voltage is different from the grid frequency. The main switch only closes ($-sw_{gr}$) when the voltage vectors overlap for a very short time.

## 3. System Description

The scheme of the considered power plant is presented in Figure 3. The analysed power system comprises the power electronic converter (PEC) with a controlled load (CL) and a fixed capacitor bank (CB). The small-scale laboratory model was built with a 7.5 kW squirrel-cage induction machine, a photo of which is presented in Figure 4. In the laboratory setup, another induction machine works as a prime mover and drives the generator. The entire control system is implemented in the microcontroller platform and integrated with the PEC control system. The grid connection is made through the grid switch $-sw_{gr}$, controlled by the common control system. The other auxiliary power switches from $-sw_1$ to $-sw_3$ are only used to change the system configuration and investigate different case studies. It should be highlighted that the auxiliary switches are not part of the final system. The grid connection is made via a 10.0 kVA laboratory transformer to match the grid and generator voltages. The laboratory transformer also ensures the proper power scale of the real system, where the power of the transformer is comparable to the generator's power. Therefore, the laboratory transformer simulates the grid with a nominal voltage equal to 185 V. The parameters of the described laboratory setup are summarised in Table 2. It should be noted that the nominal parameters of the induction machine are for motor operation mode. The power parameters for generator mode were approximately calculated and are summarised in Table 3 for better clarity. Moreover, Table 3 contains calculations for two system configurations. One column contains system power parameters for the optimal design, where the power components are adjusted to the generator's nominal voltage. In this case, the generator power can be fully utilised and transferred to the grid. However, the grid voltage in the experimental setup does not perfectly match the generator's nominal voltage. Therefore, the other column in Table 3 contains the de-rated power values of the generator and converter calculated for the laboratory grid voltage (185 V). These de-rated values ensure a fair comparison of system component powers.

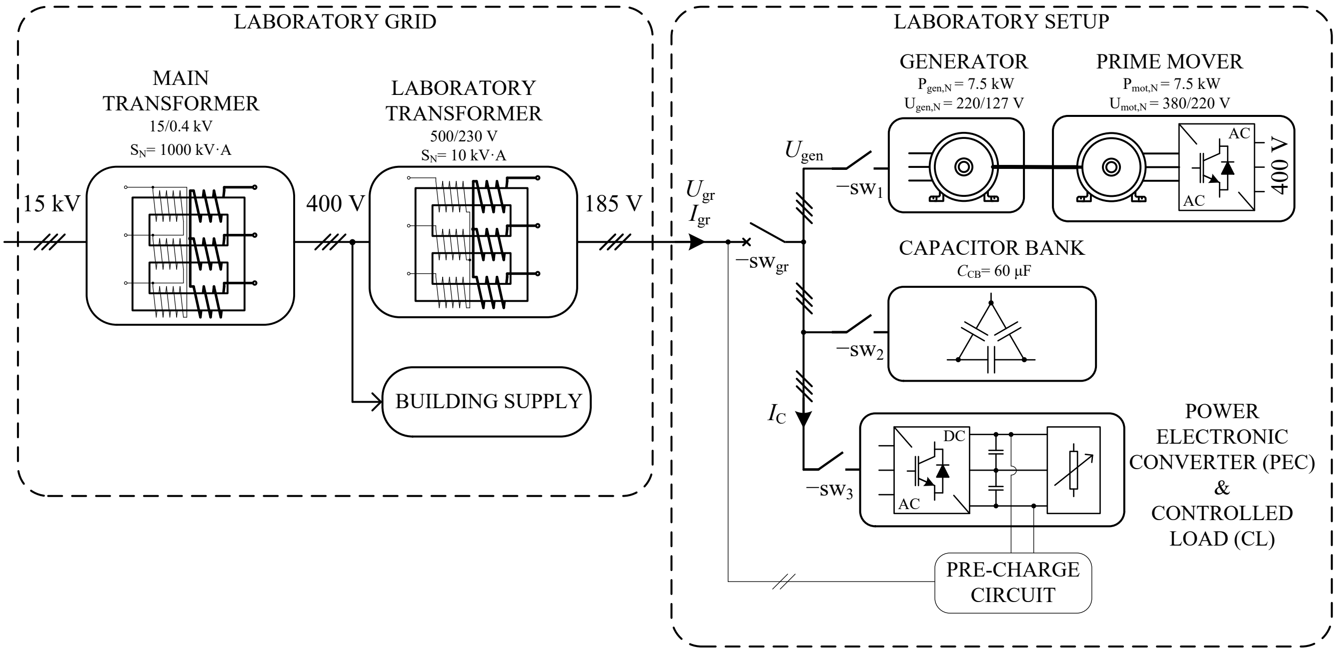


**Figure 3.** Electrical diagram of small-scale power system used in laboratory setup.

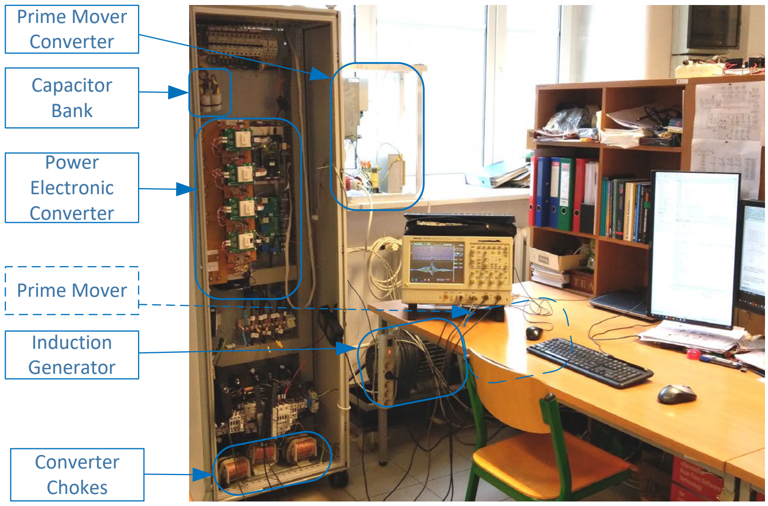


**Figure 4.** Laboratory setup of the squirrel-cage induction generator and parallel NPC converter.

**Table 2.** Parameters of system components in the laboratory setup.

| System Components | Symbol | Parameter | Value |
|---|---|---|---|
| Induction Machine used as Generator | $P_N$ | Rated mechanical power | 7.5 kW |
| | $n_N$ | Rated speed | 1450 rpm |
| | $U_N$ | Rated voltage (L-L, RMS) | 220 V |
| | $I_N$ | Rated current (RMS) | 27.1 A |
| | $f_N$ | Rated frequency | 50 Hz |
| | $\eta$ | Efficiency | 0.86 |
| | PF | Power factor | 0.84 |
| Laboratory Transformer | $S_N$ | Rated apparent power | 10 kVA |
| | $U_{PN}/U_{SN}$ | Rated primary/secondary voltage (RMS) | 500/230 V |
| | $I_{PN}/I_{SN}$ | Rated primary/secondary current (RMS) | 11.5/25 A |
| | %Z | Percentage impedance | 3.23% |

**Table 2.** *Cont.*

| System Components | Symbol | Parameter | Value |
|---|---|---|---|
| Main Transformer | $S_N$ | Rated apparent power | 1000 kVA |
| | $U_{PN}/U_{SN}$ | Rated primary/secondary voltage (RMS) | 15/0.4 kV |
| | %Z | Percentage impedance | 5.74% |
| Grid | $U_{gr,N}$ | Nominal laboratory grid voltage | 185 V |
| Power Electronic Converter | $f_S$ | Switching frequency | 10 kHz |
| | $C_D$, $C_U$ | Capacitance of the DC-link capacitors | 2.2 mF |
| | $L_C$ | Converter chokes inductance | 1.8 mH |
| | $I_{C,N}$ | Rated current (RMS) | 16 A |
| | | Rated current (RMS)—reduced power converter, software limited | 8 A |
| | $C_F$ | Capacitance of filtering capacitors | 10 uF |
| Capacitor Bank | $C_{CB}$ | Capacitance | 60 uF |
| Controlled Load | $R_U$, $R_D$ | Braking chopper resistance | 10 Ω |

**Table 3.** Approximate powers of the system components recalculated to given rated voltage values at 50 Hz.

| System Component | Symbol | Parameter | Value for Optimal System Design (220 V) | Value for the Test Setup (185 V) | Unit |
|---|---|---|---|---|---|
| Generator (Induction Machine) | $U_{gen,r}$ | Rated voltage, assumed for the generator operation mode | 220 | **185** | **V** |
| | $S_{gen,r}$ | Apparent power capability of the induction machine calculated for generator operation mode | 10.38 | **8.73** | **kVA** |
| | $P_{gen,r}$ | Active power capability of the induction machine calculated for generator operation mode | 8.72 | **7.3** | **kW** |
| | $Q_{gen,r}$ | Reactive power capability of the induction machine calculated for generator operation mode | 5.63 | **4.74** | **kvar** |
| Grid | $U_{gr,N}$ | Nominal grid voltage | 220 | **185** | **V** |
| Power Electronic Converter | $Q_C$ | Reactive power capability at given operating voltage | 5.72 | **4.81** | **kvar** |
| Reduced Power Electronic Converter (software-limited ratings) | $Q'_C$ | Reactive power capability at given operating voltage | 3.05 | **2.56** | **kvar** |
| Filtering Capacitors | $Q_f$ | Reactive power at given operating voltage | 0.45 | **0.32** | **kvar** |
| Capacitor Bank | $Q_{CB}$ | Reactive power at given operating voltage | 2.74 | **1.94** | **kvar** |

In the considered system, the prime mover (PM) drives an induction generator without speed control. The torque–speed characteristic of the prime mover $t_{PM}(\omega_{PM})$ is described as follows:

$$t_{PM}(\omega_{PM}) = T_{PM\_max}\left[1 - exp\left(-\frac{\omega_{PM\_max} - \omega_{PM}}{\Delta\omega_{PM\_int}}\right)\right] \quad (1)$$

where $t_{PM}$ is the torque of the prime mover, $T_{PM\_max}$ is the maximum torque of the prime mover, $\omega_{PM\_max}$ is the maximum speed of the prime mover, and $\Delta\omega_{PM\_int}$ defines a speed interval range, where PM torque decreases exponentially to zero value at PM maximum speed.

An adopted torque–speed function of the PM model imitates the turbine's mechanical losses and coarse guarding against runaway.

The topology of PEC and CL is presented in Figure 5. The converter is a three-leg Neutral-Point Clamped (NPC) converter, and each leg of the converter matches the corresponding terminal of the generator's stator. The three-level topology of the converter offers lower current ripples than a typical two-level topology. Therefore, the converter designed for the same current ripples and switching frequency has a reduced choke filter [15,16]. The controlled load (CL) consists of two resistors ($R_{\mathrm{U}}$ and $R_{\mathrm{D}}$) connected to the upper and lower DC-link part via IGBT transistors. The control system regulates dissipated energy using Pulse Width Modulation (PWM) for the gate signals of those transistors.

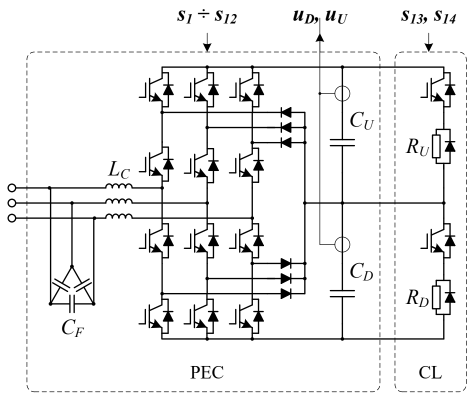


**Figure 5.** Power electronic converter (PEC) and controlled-load (CL) topologies applied in the analysed system.

The capacitor bank (CB) is connected to the generator's terminals and satisfies part of the reactive power demand of the generator, allowing for a decrease in the rated power of the PEC. The system with a converter excited generator is connected to the grid via the $-\mathrm{sw}_{\mathrm{gr}}$ contactor after synchronisation.

*Control System*

A diagram of the main control system is presented in Figure 6a. The details of the control system are explained more in Figure 6b,c. The control system controls the power electronic converter (PEC), controlled load (CL), and grid contactor ($-\mathrm{sw}_{\mathrm{gr}}$). The entire control system uses the space vector method, which is made in an $x$-$y$ coordinate frame. The phase voltages used in the control system are calculated from the measured line-to-line voltages. The analysed system is three-phase and symmetrical, where the sum of all phase voltages or currents equals zero. Therefore, the phase voltages are calculated as follows:

$$\begin{cases} u_a = \frac{2u_{ab}+u_{bc}}{3} \\ u_b = \frac{u_{bc}-u_{ab}}{3} \end{cases} \tag{2}$$

where $u_a$, $u_b$ are the voltage of phases $a$ and $b$, $u_{ab}$ is the line-to-line voltage between phases $a$ and $b$, and $u_{bc}$ is the line-to-line voltage between phases $b$ and $c$.

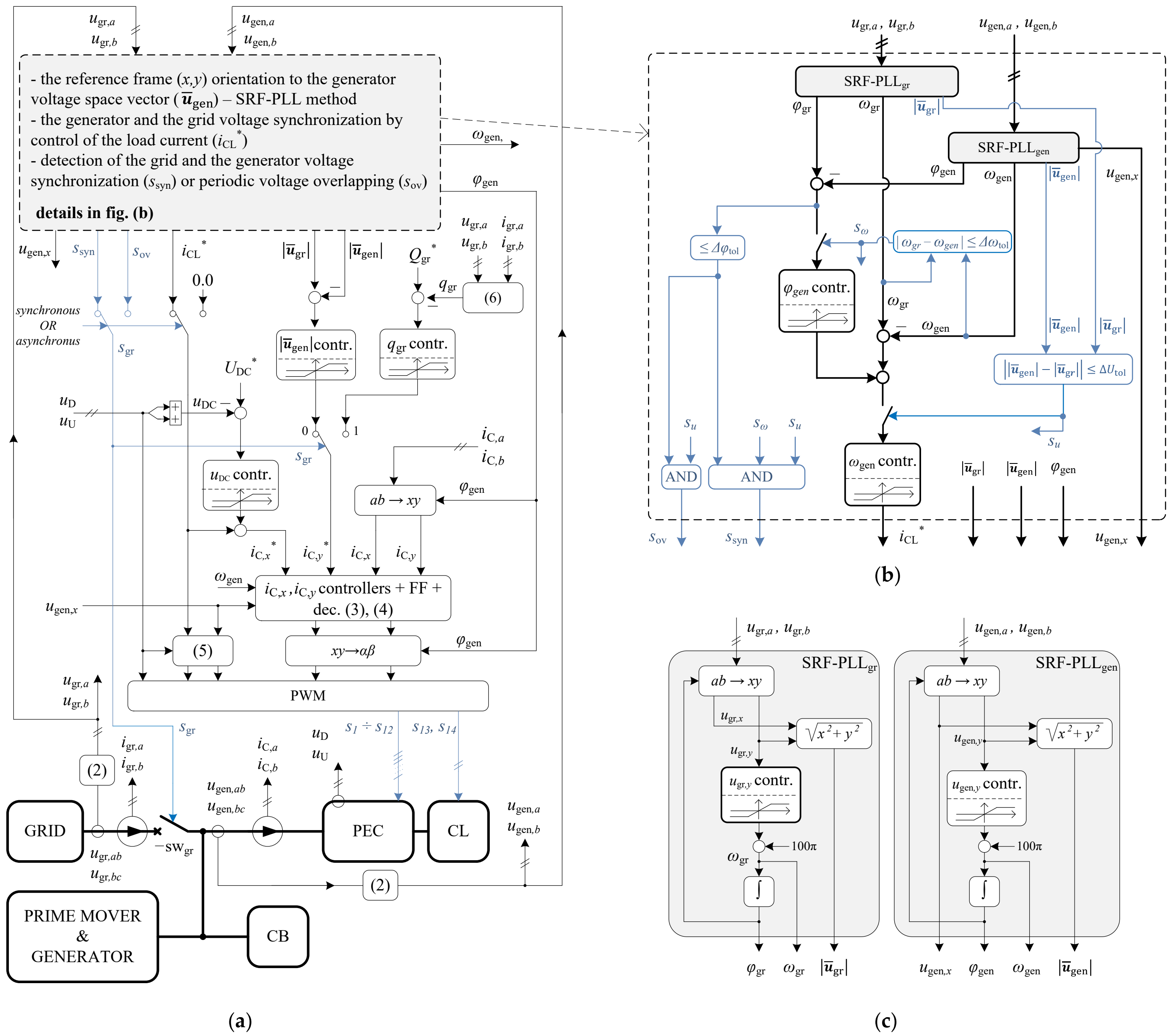


**Figure 6.** Control system of a power electronic converter applied for generator excitation and grid connection of induction generator: (**a**) main control circuit, where PEC—power electronic converter, CL—controlled load, CB—capacitor bank; (**b**) multifunctional subsystem including the reference frame orientation and voltage synchronisation; (**c**) blocks of Synchronous Reference Frame Phase-Locked Loops (SRF-PLLs) with auxiliary signal outputs.

The entire vector control is oriented in the reference frame, which rotates synchronously with the generator voltage space vector $\overline{u}_{gen}$. Thus, the $x$-coordinate of the generator voltage space vector ($u_{gen,x}$) equals the length of the space vector $|\overline{u}_{gen}|$, and $u_{gen,y}$ equals 0 [17,18]. Signals of the amplitudes, angular frequencies, and angles of the generator and grid voltage vectors are obtained using Synchronous Reference Frame Phase-Locked Loop algorithms (SRF-PLLs) [19,20], which are presented in Figure 6c.

The control system operation starts with the generator excitation process, as already explained in the general algorithm in Figure 2c. During this stage, the prime mover rotates the generator and the generator generates a small voltage value due to a remaining magnetisation flux. The SRF-PLLs obtain all required space vector parameters of the grid and generator voltages (Figure 6b). During generator-controlled excitation, the generator voltage controller (“$|\overline{\boldsymbol{u}}_{\text{gen}}|$ contr.”) has a major role. It gives a reference value of the $y$-component of the generator current ($i^*_{\text{C},y}$), which controls the reactive current supplied to the generator. The flow of the reactive current results in the increasing amplitude of the generator voltage. During this stage, the reference signal $i^*_{\text{C},x}$ is relatively low or near zero. Since the DC-bus voltage is energised, the reference converter current $i^*_{\text{C},x}$, given by the DC-bus voltage controller (“$u_{\text{DC}}$ contr.”), is relatively small. The active converter current ($i^*_{\text{C},x}$) compensates only the converter losses to keep the DC-bus voltage at the desired level. The reference value of the load current $i^*_{\text{CL}}$ is zero, because the voltage equality conditions are not fulfilled and the controller of the generator angular frequency (“$\omega_{\text{gen}}$ contr.”—Figure 6c) is not working at this moment. The reference values for the $x$, $y$ converter current components are fed to the current controller block in Figure 6a. The block contains the PI current controllers with anti-windup and the decoupling between the converter current components and the grid voltage feedforward (FF). Thus, the reference signals of the $x$- and $y$-components of the converter voltage are obtained from Equations (3) and (4).

$$u^*_{\text{C},x} = k_I\left(i^*_{\text{C},x} - i_{\text{C},x}\right) + \frac{k_I}{T_I}\int\left(i^*_{\text{C},x} - i_{\text{C},x}\right)\text{d}t + u_{\text{gen},x} + \omega_{\text{gen}}L_{\text{C}}i_{\text{C},y} \tag{3}$$

$$u^*_{\text{C},y} = k_I\left(i^*_{\text{C},y} - i_{\text{C},y}\right) + \frac{k_I}{T_I}\int\left(i^*_{\text{C},y} - i_{\text{C},y}\right)\text{d}t - \omega_{\text{gen}}L_{\text{C}}i_{\text{C},x} \tag{4}$$

where $\omega_{\text{gen}}$ is the generator angular frequency, $L_{\text{C}}$ is an inductance of the converter’s choke, and $k_{\text{I}}$, $T_{\text{I}}$ are the gain and integration time of the PI current controllers.

When the generator voltage amplitude (vector module) reaches the grid voltage amplitude, the synchronisation process starts, assuming the synchronised method is selected. During the synchronisation, the voltage vector equality condition is fulfilled, so the generator angular frequency controller (“$\omega_{\text{gen}}$ contr.”) works (Figure 6b). It produces a non-zero reference value of the load current $i^*_{\text{CL}}$, which is part of the reference generator current $i^*_{\text{C},x}$ and results in loading the generator with active current. The value of the reference load current $i^*_{\text{CL}}$ is also fed to a block (5). This block produces a duty cycle signal to the PWM block to dissipate the same quantity of power in passive load as it is taken from the generator. The duty cycle signals are determined by Equation (5), as follows:

$$d_{13} = d_{14} = \sqrt{\frac{i^*_{\text{CL}} \cdot u_{\text{gen},x} \cdot (R_{\text{D}} + R_{\text{U}})}{(u_{\text{D}} + u_{\text{U}})^2}} \tag{5}$$

where $i^*_{\text{CL}}$ is a reference load current, which is the output of the generator frequency controller; $R_{\text{D}}$, $R_{\text{U}}$ are braking chopper resistances; and $u_{\text{D}}$, $u_{\text{U}}$ are the voltages of the upper and lower capacitor in the DC-link.

The loading of the generator results in the decreasing angular frequency of the generator voltage. When the angular frequency of the generator voltage matches the grid voltage angular frequency, the generator voltage phase controller (“$\varphi_{\text{gen}}$ contr.”) starts operation and equalises the phases of the grid and generator voltages. The control system sets the synchronisation signal, $s_{\text{syn}}$, when the voltage vectors are synchronised (equal phases with given tolerance). The synchronisation signal activates the main switch ($-\text{sw}_{\text{gr}}$) and the generator is connected to the grid without any inrush current; this will be shown in the Laboratory Test Results section. After the connection, the reference signal $i^*_{\text{C},y}$ for the current controller block is switched to the grid reactive power controller (“$q_{\text{gr}}$ contr.”). The current value of the $q_{\text{gr}}$ component is calculated using the coordinates of the grid voltage and grid current vectors in stationary coordinates ($\alpha$,$\beta$), as follows [21]:

$$q_{\text{gr}} = u_{\text{gr},\beta}i_{\text{gr},\alpha} - u_{\text{gr},\alpha}i_{\text{gr},\beta} \tag{6}$$

At this moment, the generator operates in normal mode and the converter controls the reactive power delivered to the grid depending on the reference value $Q_{gr}^{*}$.

The control of the asynchronous connection method is analogical, but the generator loading process is omitted. The signal switch in Figure 6a is in a position whereby $i_{CL}^{*}$ is always zero. Therefore, the controlled load does not work and the signal from the generator angular frequency controller ("$\omega_{gen}$ contr."—Figure 6b) does not affect the system's operation. The control system only detects the overlapping of the grid and generator vectors and sets the overlapping signal $s_{ov}$ to connect the main grid switch ($-sw_{gr}$).

## 4. Capacitance Consideration for the Capacitor Bank

The reactive power demand of an induction machine depends on the RMS value and frequency of the voltage at the machine's terminals and the machine's active power [22]. During the grid operation of an induction generator, the reactive power taken from the grid depends only on the active power delivered to the grid because the RMS value and frequency of the grid voltage can be considered constant. The relation of the reactive power consumed by the generator as a function of the active power produced during grid operation is shown in Figure 7. The reactive power's dependence on an induction machine's active power is not linear. The reactive power falls to about 0.8 of the machine's rated reactive power for small active power values. Hence, it is reasonable to satisfy part of the reactive power demand of the induction machine with a fixed capacitor bank, thus reducing the rated power of the converter.

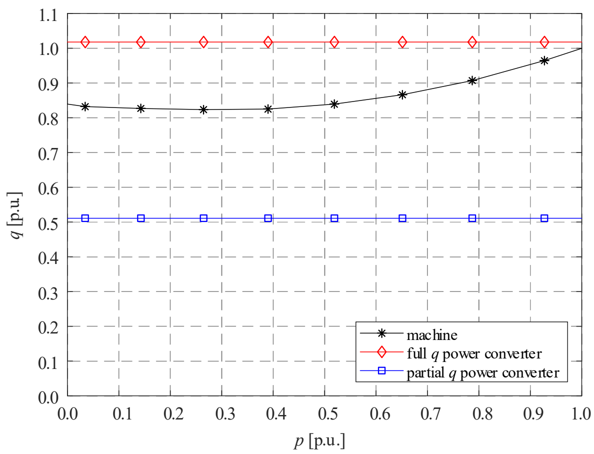


**Figure 7.** The dependency of the reactive generator power as a function of its active power. Additionally, the figure presents the rated power lines of the full and partial power converters at 220 V and 50 Hz.

Grid-connected induction generators must operate with a reactive power compensator. The compensator cannot deliver more reactive power than the generator demands. This requirement leads to the formula for the first capacitance limit, as follows:

$$C_{max1} < \frac{Q_{gen\_min}}{3\omega_{gr}{U_{gr}}^2} \quad (7)$$

where $C_{max1}$ is the maximal capacitance of the capacitors bank, which does not deliver reactive power to the grid; $Q_{gen\_min}$ is the minimum value of the generator's reactive power taken from the grid under different active power; $\omega_{gr}$ is the angular frequency of the grid; and $U_{gr}$ is the line-to-line voltage of the grid.

The dependence of a generator's reactive power on its active power is not the only factor affecting the capacitance of the capacitor bank (CB). The capacitance selection must consider the uncontrolled excitation of a rotating induction generator with a fixed capacitor bank. Figure 8a presents the magnetisation characteristic of the induction generator at 50 Hz with the capacitor bank voltage lines for 70 µF and 105 µF at Δ-connection. The graphically presented characteristics show that a 105 µF capacitor bank results in the intersection of the capacitor bank's voltage characteristic with the machine's magnetisation curve, which ultimately allows the unloaded generator to self-excite up to the phase voltage of 125 V. In contrast, the capacitance of 70 µF is still not sufficient to initiate the phenomenon of self-excitation of an induction generator at 50 Hz. The maximal capacitance of the capacitor bank (CB), which does not cause the dangerous phenomenon of generator self-excitation, can be determined by Equation (8) [22,23].

$$C_{\mathrm{max2}} < \frac{1}{3(L_{\sigma\mathrm{S}} + L_{\mu,\mathrm{max}})\omega_{\mathrm{gen},0}{}^2} \tag{8}$$

where $C_{\mathrm{max2}}$ is the maximal capacitance of the capacitor bank, which does not cause self-excitation; $\omega_{\mathrm{gen},0}$ is the maximum angular frequency of the induction generator; and $L_{\sigma\mathrm{S}}$, $L_{\mu,\mathrm{max}}$ are the stator leakage and maximum value of the magnetising inductance.

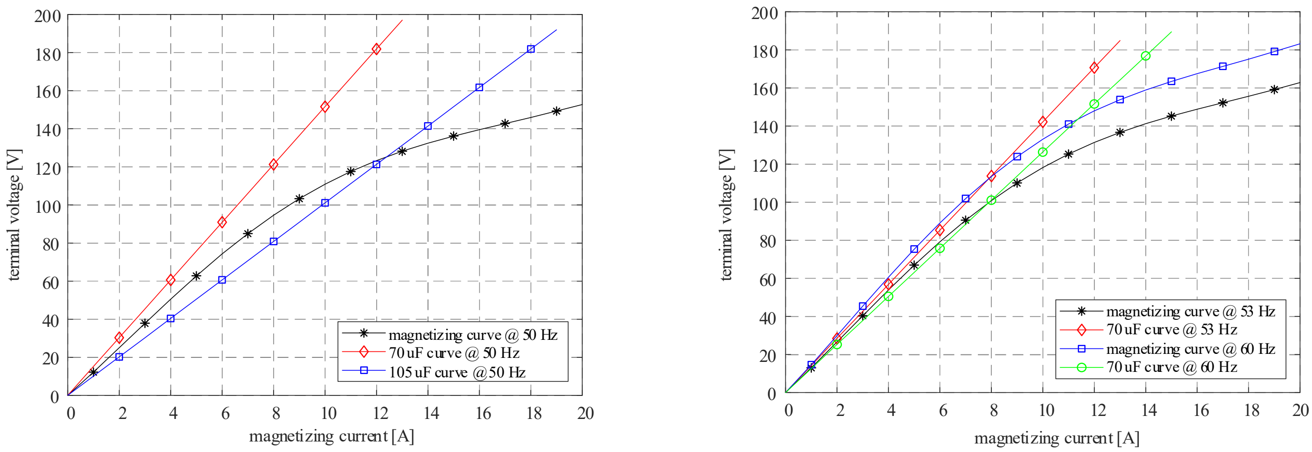


(**a**) (**b**)

**Figure 8.** Magnetisation curve of an induction generator (**a**) at 50 Hz with the capacitor bank voltage line for 70 µF and 105 µF and (**b**) at different frequencies with the capacitor bank voltage lines for 70 µF.

The maximum value of the magnetising inductance is calculated as follows:

$$L_{\mu,\mathrm{max}} = \max\{L_\mu(I_\mu)\},\ I_\mu \in \langle 0.0; \mathrm{I}_{\mathrm{gen,N}} \rangle \tag{9}$$

where $\mathrm{I}_{\mathrm{gen.N}}$ is the nominal value of the generator current (the same as the nominal current in motor operating mode).

Further, in the no-load operation of an induction generator, the machine slip is close to zero, and the maximum frequency of the generated voltage is related to the maximum speed of the prime mover. It can be described as follows:

$$\omega_{\mathrm{gen},0} = p_{\mathrm{B}}\omega_{\mathrm{PM\_max}} \tag{10}$$

Figure 6b shows the magnetisation curves of the induction generator and the voltage lines of the 70 µF capacitor bank at 53 Hz and 60 Hz. The magnetisation curve of the induction generator and the voltage line of the 70 µF capacitor bank at 53 Hz (~1600 rpm) have no intersection points. This fact ensures that the 70 µF capacitor bank can be used as a partial source of the generator's reactive power without the risk of uncontrolled self-excitation. A further increase in the generator frequency up to 60 Hz could lead to the initiation of a self-excitation, which is an undesirable and dangerous phenomenon. Thus, the capacitor bank should be disconnected from the rotating generator in the absence of the working converter, or the capacitance of the capacitor bank should be reduced.

Finally, the total capacitance in the system should be as high as possible, but cannot exceed the limit according to the following formula:

$$(C_{CB} + C_F) \leq \min\{C_{max1}, C_{max2}\} \quad (11)$$

The calculated capacitance limits are given in Table 4, which confirms that the total capacitance of 70 uF is within the allowable limits. A capacitor bank with 60 µF capacitors at Δ-connection together with filtering capacitors at 10 µF meets 55% of the rated reactive power demand of an induction generator at 220 V and 50 Hz (Table 3). This allows the rated power of the converter to be reduced to approximately half of the rated reactive power of the generator.

**Table 4.** Calculated maximal capacitances for two values of system voltages at 50 Hz.

| Line–Line Voltage $U_{gen}$ | Capacitance $C_{max1}$ | Capacitance $C_{max2}$ | Applied Total Capacitances ($C_F$ + $C_{CB}$) |
|---|---|---|---|
| 220 V | 100 µF | 74 µF | 70 µF |
| 185 V | 120 µF | 74 µF | 70 µF |

## 5. Experiment Description

The proposed method and system configuration were tested on a reduced-scale laboratory model of the power system, which was described in the section "System Description". The experiments were performed for five different study cases, summarised in Table 5. The first case concerns the direct connection of the unexcited generator to the grid. This case aims to show the disturbances created in the typical power system related to the laboratory setup. The second objective is to use the results as a reference for other study cases. For this case, the converter and the capacitor bank were disconnected from the systems by opening the auxiliary power switches $-sw_2$ and $-sw_3$ (Figure 4). Next, the two experiments for the converter-synchronised connection were designed to show the advantages of this connection method (case 2 and case 3). The synchronised method concerns two system configurations. For both configurations, the converter was connected to the system (the auxiliary power switch $-sw_2$ is closed—Figure 4). The first configuration (case 2) has no capacitor bank, and the auxiliary power switch $-sw_3$ is open (Figure 4). The second configuration (case 3) is the proposed system, which has a connected capacitor bank ($-sw_3$ is closed—Figure 4). In this case, the converter current was limited in the software to prove that the system can operate correctly with the reduced power converter. The system has a total capacitance of 70 uF since the capacitor bank gives 60 uF and an additional 10 µF comes from a filtering capacitor $C_F$ in the converter. The last experimental cases were designed for the second generator connection method—the asynchronous approach. This method was also validated using two system configuration variants: with a capacitor bank (case 4), and with a reduced power converter (software-limited) and a capacitor bank (case 5). The hardware configuration is analogical to case 2 and 3, but the control system does not use a controlled load. For all cases, the maximum torque and speed of the prime mover were limited to 8 Nm ($T_{PM\_max}$) and 1600 rpm ($\omega_{PM\_max}$ = 167.5 rad/s), respectively.

**Table 5.** Summary of experimental study cases.

| Case No. | Generator Connection Method | System Configuration | | | |
|---|---|---|---|---|---|
| | | Configuration Name | Converter | Controlled Load | Capacitor Bank |
| 1 | Direct | Typical | No | No | No |
| 2 | Synchronised | Introduced in [14] | Yes | Yes | No |
| **3** | **Synchronised** | **Proposed** | **Reduced Size** | **Yes** | **Yes** |
| 4 | Asynchronous | Introduced in [13] | Yes | No | No |
| **5** | **Asynchronous** | **Proposed** | **Reduced Size** | **No** | **Yes** |

## 6. Laboratory Tests Results

The experimental result of the direct generator-to-grid connection process is presented in Figure 9 (case 1). For this case study, the maximum speed of the prime mover was limited to 1600 rpm. Therefore, the difference in the voltage frequency between the grid voltage and the generator voltage was 3 Hz. The generator was connected at random moment, as in a typical power system with an induction generator. At the time of direct grid connection (Figure 9), an inrush grid current appeared. It had a value of almost 200 A in the magnitude of the current vector, which is about five times higher than the rated value. Furthermore, the inrush current caused an undesired grid voltage drop of about 30%.

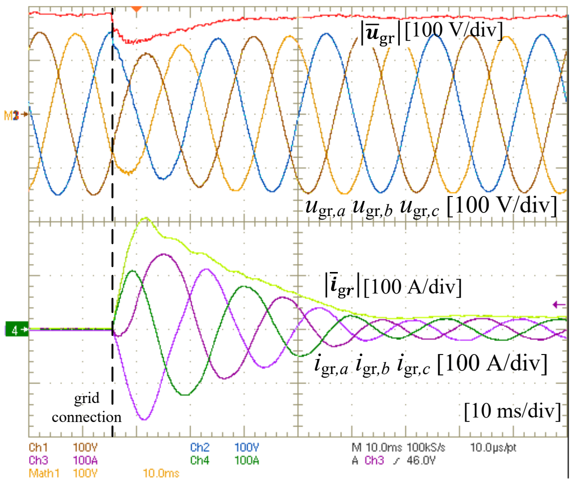


**Figure 9.** Currents and voltages for direct grid connection of a squirrel-cage induction generator at a speed equal to 1600 rpm in a laboratory small scale setup—case 1 [13].

The advantages of the synchronised connection method using the converter are presented in Figure 10. The validation results of the system variant without the capacitor bank are presented in Figure 10a. The validation results of the proposed system, with the reduced power converter and the 60 µF capacitor bank (70 µF of total capacitance), are presented in Figure 10b. Both figures present the waveforms of the grid and the converter currents during the generator-to-grid connection process. The process is split into three time intervals. The first interval is the generator excitation process. Figure 10 begins at the state when the generator has already been excited. The entire excitation process driven by the converter is presented in Figure 11 and concerns the system with the 60 µF capacitor bank. During this interval, the generator has super-synchronous speed, the generator is islanding, and the power converter provides reactive power to the generator to build up the proper voltage amplitude. When the generator is excited, the synchronisation process of the generator voltage with the grid voltage starts (Interval 2 in Figure 10). During the synchronisation interval, the converter instantaneously loads the generator using the controlled load. The prime mover speed and generator frequency become lower. When the frequency and phase of the generator voltage match the grid voltage, the circuit breaker connects the excited generator to the grid. Then, the converter stops to load the generator and the generator supplies active power to the gird. Finally, the power converter precisely satisfies the reactive power demand of the generator (Interval 3 in Figure 10). The results clearly show that the synchronised generator-to-grid connection controlled by the converter effectively eliminates the inrush grid currents, which was the main drawback of the direct generator-to-grid connection method (Figure 9). The results presented in Figure 10b prove that converter-driven synchronisation also works with the reduced size of the converter. The amplitude of the converter current ($i_C$) is reduced from 18 A (Figure 10a) to 6 A (Figure 10b), which allows for a reduction in the apparent power, size, and cost of the power converter. The effect of the capacitor bank application is visible in the first interval in Figure 10b. The converter current is reduced to a few amperes because the converter delivers only a fraction of the reactive power required by the generator. In the third interval in Figure 10b, the converter works as a reactive power compensator and must provide more reactive power than in Interval 1. The active power generation process causes a higher demand for reactive power, according to the characteristic presented previously in Figure 7. Another factor influencing reactive power is the lower angular frequency and related changes in generator and capacitor reactance.

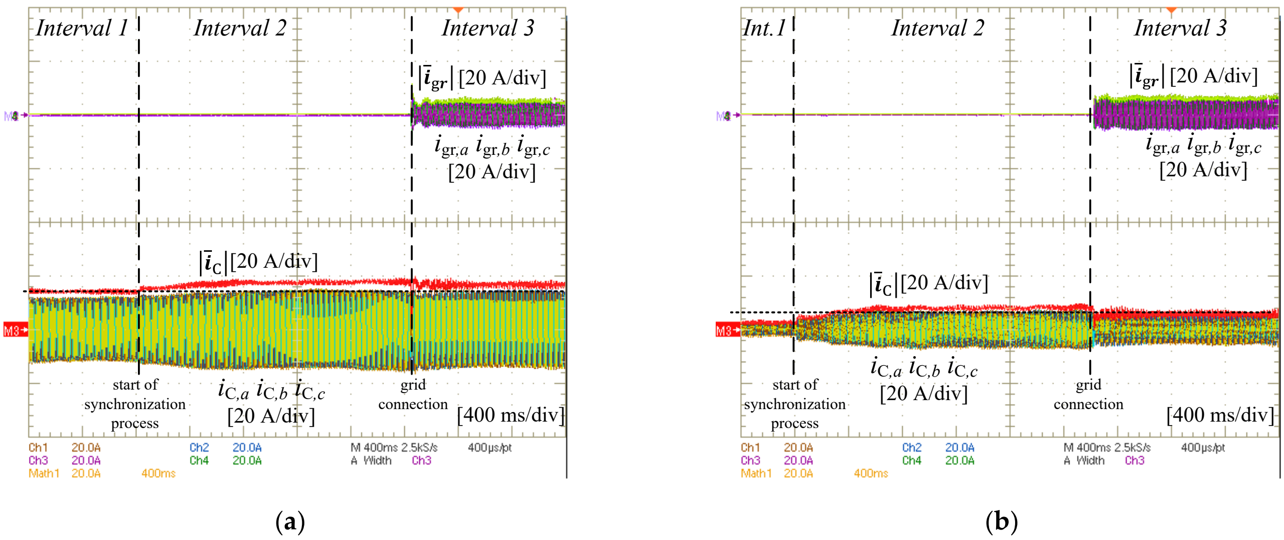


**Figure 10.** Laboratory test results for generator-to-grid connection using the converter loading method: (**a**) grid and converter currents for full power converter—case 2 [14]; (**b**) grid and converter currents for reduced power of converter—case 3.

The proposed power system configuration with the control algorithm also allows the asynchronous generator-to-grid connection method to be used. The laboratory validation results for this connection method are presented in Figure 12. The figure presents two variants of the system configuration: the power system with a filtering capacitor only (Figure 12a), and the system with a 70 µF capacitor bank and a reduced converter power. The presented process of connecting the generator to the grid begins with the already-excited generator in the same way as previously discussed and presented in Figure 11. The moment of generator-to-grid connection is marked in Figure 12 and is activated by the control system when the grid and generator voltage phases match one another. However, in this case, the angular frequencies of the grid and generator voltages are different, resulting in an insignificant transient state after the connection. During the transient state, the generator speed approaches a new operation point, resulting from the prime mover torque characteristic. Also, the grid current amplitude rises temporarily to 33 A, and the converter delivers the maximum allowable current according to its amplitude limitation (11 A). When the transient state vanishes, the generator provides active power to the grid, and the converter satisfies the reactive power of the generator. The grid current reaches an amplitude value of about 4 A, which is the same as in the previously presented method in Figure 10, but it is hardly visible due to the waveform scale. The main difference between the two system configurations in Figure 12a,b is the value of the converter current, which is reduced in Figure 12b by the application of the capacitor bank.

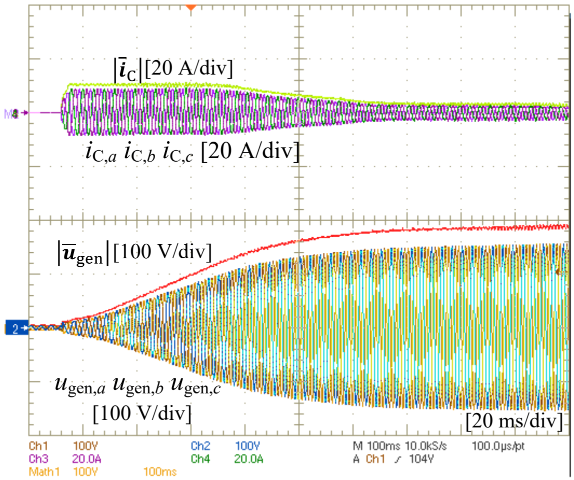


**Figure 11.** Laboratory test results for the converter-controlled excitation of the induction generator at a speed equal to 1600 rpm: generator voltages and converter currents for reduced power converter.

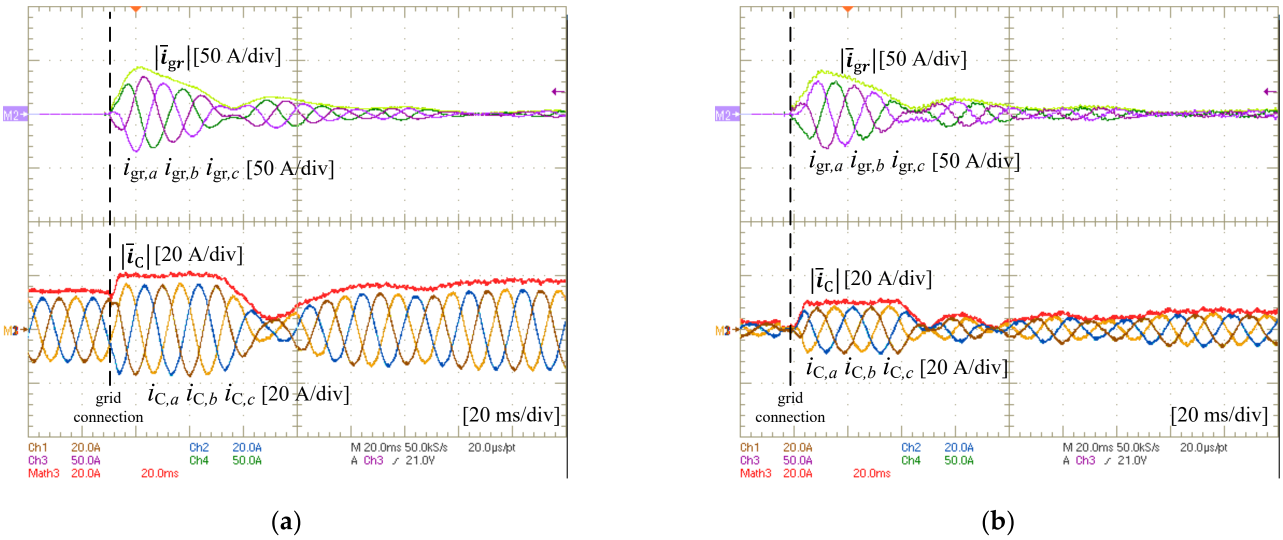


**Figure 12.** Laboratory test results for asynchronous generator-to-grid connection method at generator speed equal to 1600 rpm: (**a**) generator voltages and converter currents for full power converter—case 4 [13]; (**b**) generator voltages and converter currents for half power converter—case 5.

## 7. Conclusions

This paper presents a control system for the grid connection of a squirrel-cage induction generator using a power electronic converter, which was experimentally validated. The proposed control system can use two different generator-to-grid connection methods, significantly reducing disturbances in the grid/microgrid compared with the often-used direct connection method. The control system of the generator connection process was improved by adding a fixed capacitor bank and power electronic converter in parallel to the generator's terminals. The proposed modification reduces the power electronic converter's rated power without compromising system performance. This modification further leads to a system cost reduction, assuming that the additional capacitor bank cost is lower than the increased power capability (size) of the power converter. The connection system with the power electronic converter still has the capability of the continuous compensation of reactive power for the entire range of active power produced by the generator. Another advantage of the proposed system is the high quality of the grid voltage during generator-to-grid connection, which minimises disturbances in the grid.

The proposed connection system was validated using a small-scale laboratory setup. The experimental results clearly show that adding a capacitor bank reduces the converter currents, and the converter-driven connection process is performed correctly. The only drawback of converter power reduction might be a longer connection process in the case of the method that involves generator loading by the converter. However, this does not matter in practice because the connection lasts a few seconds. Further reduction of the system is possible by eliminating the controlled load connected to the converter, but this leads to the converter loading method being eliminated. Then, only the asynchronous connection method might be used at the cost of limited disturbance in the grid after the moment of generator connection. However, this disturbance can be ignored, considering the value of the transient grid current and the nominal value of the generator current.

**Author Contributions:** Conceptualisation, methodology, and software, D.A.G.; validation, D.A.G. and G.D.; formal analysis, G.I.; investigation, D.A.G. and G.D.; writing—original draft preparation, D.A.G. and G.D.; writing—review and editing, G.I.; visualisation, D.A.G. and G.D.; supervision, G.I. All authors have read and agreed to the published version of the manuscript.

**Funding:** This research was partially funded by the statutory fund of the Electrical Drive Division within the Institute of Control and Industrial Electronics, Faculty of Electrical Engineering, Warsaw University of Technology.

**Data Availability Statement:** The original contributions presented in this study are included in the article. Further enquiries can be directed to the corresponding authors.

**Conflicts of Interest:** The authors declare no conflicts of interest.

## List of Symbols and Acronyms

| | |
|---|---|
| $p_{\mathrm{B}}$ | pole pairs of the induction generator |
| $C_{\mathrm{BC}}$ | capacitor in the capacitor bank for support excitation |
| $C_{\mathrm{D}}$, $C_{\mathrm{U}}$ | capacitors in the DC-link of the power converter |
| $C_{\mathrm{F}}$ | filtering capacitor in the AC side of the power converter |
| $C_{\mathrm{max1}}$ | maximum value of the capacitance, which can satisfy the reactive power demand of the generator |
| $C_{\mathrm{max2}}$ | maximum value of the capacitance, which does not cause self-excitation |
| $d_{13}$, $d_{14}$ | duty cycle of the gating signals of the braking chopper transistors |
| $f_{\mathrm{s}}$ | switching frequency of the power converter |
| $\mathrm{I}_{\mathrm{gen,N}}$ | nominal value of the generator current |
| $i_{\mathrm{C,a}}$, $i_{\mathrm{C,b}}$ | converter currents: a and b phases, respectively |
| $i_{\mathrm{C,x}}$, $i_{\mathrm{C,y}}$ | x and y coordinates of the converter current space vector |
| $i^{*}_{\mathrm{C,x}}$, $i^{*}_{\mathrm{C,y}}$ | reference values of x and y coordinates of the converter current space vector |
| $i^{*}_{\mathrm{CL}}$ | reference value of the load current |
| $i_{\mathrm{gr,x}}$, $i_{\mathrm{gr,y}}$ | x and y coordinates of the grid current space vector, respectively |
| $I_{\mu}$ | magnetising current in the induction machine |
| $k_{\mathrm{I}}$, $T_{\mathrm{I}}$ | gain and integration time of the PI current controllers, respectively |
| $L_{\mathrm{C}}$ | inductance in the filtering chokes in the AC side of the power converter |
| $L_{\sigma\mathrm{s}}$ | leakage stator inductance |
| $L_{\mu}$ | magnetising inductance |

| | |
|---|---|
| $Q_{gen\_min}$ | minimum value of the generator's reactive power taken from the grid under different active power |
| $q_{\mathrm{gr}}$ | q component of instantaneous grid power |
| $Q^*_{\mathrm{gr}}$ | reference value of q component of instantaneous grid power |
| $R_{\mathrm{D}}$, $R_{\mathrm{U}}$ | resistors for dissipation energy in lower and upper braking choppers, respectively |
| $s_1$–$s_{14}$ | gating signals of transistors in the power converter and braking choppers |
| $s_{\mathrm{gr}}$ | gating signal to close grid power switch |
| $s_{\mathrm{ov}}$ | synchronisation signal for asynchronous connection algorithm |
| $s_{\mathrm{syn}}$ | synchronisation signal for synchronous connection algorithm |
| $-\mathrm{sw}_1$ | generator switch |
| $-\mathrm{sw}_2$ | capacitor bank switch |
| $-\mathrm{sw}_3$ | converter switch |
| $-\mathrm{sw}_{\mathrm{gr}}$ | grid switch |
| $t_{\mathrm{PM}}$ | torque of a prime mover |
| $T_{\mathrm{PM\_max}}$ | maximum torque of a prime mover |
| $u^*_{\mathrm{C,x}}$, $u^*_{\mathrm{C,y}}$ | reference values of x and y coordinates of the converter voltage space vector |
| $u_{\mathrm{D}}$, $u_{\mathrm{U}}$ | voltages on the DC-link capacitors $C_{\mathrm{D}}$ and $C_{\mathrm{U}}$, respectively |
| $u_{\mathrm{DC}}$ | DC-link voltage |
| $U^*_{\mathrm{DC}}$ | reference value of DC-link voltage |
| $U_{\mathrm{gen}}$ | RMS line-to-line value of generator grid phase voltage |
| $\bar{\boldsymbol{u}}_{\mathrm{gen}}$, | generator voltage space vector |
| $\lvert\bar{\boldsymbol{u}}_{\mathrm{gen}}\rvert$ | length of the generator voltage space vector |
| $u_{\mathrm{gen,a}}$, $u_{\mathrm{gen,b}}$ | generator phase voltages: a and b phases, respectively |
| $u_{\mathrm{gen,x}}$, $u_{\mathrm{gen,y}}$ | x and y coordinates of the generator voltage space vector |
| $U_{\mathrm{gr}}$ | RMS line-to-line value of grid phase voltage |
| $\bar{\boldsymbol{u}}_{\mathrm{gr}}$ | grid voltage space vector |
| $\lvert\bar{\boldsymbol{u}}_{\mathrm{gr}}\rvert$ | length of the grid voltage space vector |
| $u_{\mathrm{gr,a}}$, $u_{\mathrm{gr,b}}$ | grid phase voltages: a and b phases, respectively |
| $u_{\mathrm{gr,x}}$, $u_{\mathrm{gr,y}}$ | x and y coordinates of the grid voltage space vector |
| $\Delta\varphi_{\mathrm{tol}}$ | tolerance of the phases of the generator and grid voltage vectors |
| $\Delta U_{\mathrm{tol}}$ | tolerance of the lengths of the generator and grid voltage vectors |
| $\Delta\omega_{\mathrm{tol}}$ | tolerance of the angular frequencies of the generator and grid voltages |
| $\varphi_{\mathrm{gen}}$ | angle of generator vector voltage |
| $\varphi_{\mathrm{gr}}$ | angle of grid vector voltage |
| $\omega_{\mathrm{gen}}$ | angular frequency of generator voltage |
| $\omega_{\mathrm{gr}}$ | angular frequency of grid voltage |
| $\omega_{\mathrm{gen,0}}$ | maximum angular frequency of the induction generator |
| $\omega_{\mathrm{PM}}$ | angular speed of prime mover |
| $\omega_{\mathrm{PM\_max}}$ | maximum angular speed of prime mover |
| CB | capacitor bank |
| CL | controlled load |
| FF | feedforward |
| PEC | power electronic converter |
| PM | prime mover |
| "$q_{\mathrm{gr}}$ contr." | controller of the grid reactive power |
| SCIG | squirrel-cage induction generator |
| SRF-PLL$_{\mathrm{gen}}$ | Synchronous Reference Frame Phase-Locked Loop algorithm adopted for generator voltages |
| SRF-PLL$_{\mathrm{gr}}$ | Synchronous Reference Frame Phase-Locked Loop algorithm adopted for grid voltages |
| "$u_{\mathrm{DC}}$ contr." | controller of the DC-link voltage |
| $\lvert\bar{u}_{\mathrm{gen}}\rvert$ contr." | controller of the generator voltage amplitude |
| "$u_{\mathrm{gen,y}}$ contr." | controller of the y component of the generator voltage vector |

| | |
|---|---|
| "$u_{gr,y}$ contr." | controller of the y component of the grid voltage vector |
| "$\varphi_{gen}$ contr." | controller of the phase of generator voltage |
| "$\omega_{gen}$ contr." | controller of the angular frequency of generator voltage |

## References


1. Gębczyk, K.; Grąkowski, Ł. Analysis of the autonomous operation of an induction generator working in a small hydropower plant. *Przeglad Elektrotechniczny.* **2019**, *95*, 76–79. [CrossRef]
2. Trairat, P.; Somkun, S.; Kaewchum, T.; Suriwong, T.; Maneechot, P.; Panpho, T.; Wansungnern, W.; Banthuek, S.; Prasit, B.; Kiatsiriroat, T. Grid Integration of Livestock Biogas Using Self-Excited Induction Generator and Spark-Ignition Engine. *Energies* **2023**, *16*, 4963. [CrossRef]
3. Silva, E.O.; Vanço, W.E.; Guimarães, G.C. A Technical and Economic Project Analysis of Asynchronous Technology in Distributed Generation Using Methane Gas from Pig Farms. *IEEE Access* **2020**, *8*, 36140–36153. [CrossRef]
4. Gorski, D.A. Analysis of squirrel-cage induction generator start-up supported by reactive power compensator. *COMPEL-Int. J. Comput. Math. Electr. Electron. Eng.* **2020**, *39*, 265–278. [CrossRef]
5. German-Galkin, S.; Tarnapowicz, D. Tests of the Ship's Cage Induction Generator with the DC Electrical Network. In Proceedings of the 19th International Conference on Mechatronics, Mechatronika, Prague, 2–4 December 2020.
6. Mihet-Popa, L.; Blaabjerg, F.; Boldea, I. Wind Turbine Generator Modeling and Simulation Where Rotational Speed is the Controlled Variable. *IEEE Trans. Ind. Appl.* **2004**, *40*, 3–10. [CrossRef]
7. Varalakshmi, K.; Bharathi, K.; Himaja, T. Study of Soft-Starter based Induction Generator for Wind Energy Conversion System. In Proceedings of the 2021 Asian Conference on Innovation in Technology (ASIANCON), Pune, India, 27–29 August 2021.
8. Prapurt, N.; Kinnares, V. Single-Phase Grid Connected Induction Generator with Soft Starting and Power Quality Improvement. In Proceedings of the 25th International Conference on Electrical Machines and Systems (ICEMS), Chiang Mai, Thailand, 29 November–2 December 2022.
9. Yamada, H.; Hanamoto, T. A Novel Method of Suppressing Inrush Currents of Squirrel-cage Induction Machine using Matrix Converter in Wind Power Generation Systems. In Proceedings of the International Conference on Renewable Energy Research and Applications ICRERA 2012, Nagasaki, Japan, 11–14 November 2012.
10. Sikorski, A.; Kuzma, A. Cooperation of induction squirrel-cage generator with grid connected AC/DC/AC converter. *Bull. Pol. Acad. Sci.* **2009**, *57*, 317–322. [CrossRef]
11. Kasprowicz, A.B.; Husev, O.; Strzelecki, R. Induction Generator with Direct Control and a Limited Number of Measurements on the Side of the Converter Connected to the Power Grid. *Energies* **2023**, *16*, 63. [CrossRef]
12. Mostafa, M.A.; El-Hay, E.A.; Elkholy, M.M. An overview and case study of recent low voltage ride through methods for wind energy conversion system. *Renew. Sustain. Energy Rev.* **2023**, *183*, 113521. [CrossRef]
13. Gorski, D.A.; Iwanski, G. Asynchronous grid connection of a cage induction generator excited by a power electronic converter. *IEEE Trans. Energy Convers.* **2021**, *36*, 63–70. [CrossRef]
14. Gorski, D.A.; Balkowiec, T.; Koczara, W. Grid Connection of a Converter Controlled Squirrel-Cage Induction Generator. In Proceedings of the 2018 7th International Conference on Renewable Energy Research and Applications (ICRERA), Paris, France, 14–17 October 2018; pp. 348–353.
15. Reddy, G.M.; Manohar, T.G. Multi Level Inverter Based STATCOM for Grid Connected Wind Energy Conversion System. *Int. J. Renew. Energy Res.* **2017**, *7*, 80–87.
16. Boulouiha, H.M.; Allali, A.; Laouer, M.; Tahri, A.; Denai, M.; Draou, A. Direct torque control of multilevel SVPWM inverter in variable speed SCIG-based wind energy conversion system. *Renew. Energy* **2015**, *80*, 140–152. [CrossRef]
17. Tępiński, J.; Wiśniewski, J.; Koczara, W. Reactive power compensator of hydro induction generator. In Proceedings of the 7th International Conference and Exhibition on Ecological Vehicles and Renewable Energies EVER 2012, Monte Carlo, Monaco, 22–25 March 2012.
18. Wiśniewski, J.; Koczara, W. Follow-up control of variable reactive power of cage induction generator driven by wind turbine. In Proceedings of the 8th International Conference and Exhibition on Ecological Vehicles and Renewable Energies EVER 2013, Monte Carlo, Monaco, 27–30 March 2013; pp. 1–6.
19. Teodorescu, R.; Liserre, M.; Rodriguez, P. Grid Synchronization in Three-Phase Power Converters. In *Grid Converters for Photovoltaic and Wind Power Systems*; John Wiley & Sons: Chichester, UK, 2011.
20. Guo, X.-Q.; Wu, W.-Y.; Gu, H.-R. Phase locked loop and synchronization methods for grid interfaced converters: A review. *Przeglad Elektrotechniczny.* **2011**, 182–187.
21. Benysek, G.; Pasko, M. Power Theories Applications to Control Active Compensators. In *Power Theories for Improved Power Quality*; Springer: London, UK, 2012.

22. Simoes, M.G.; Farret, F.A. *Modeling and Analysis with Induction Generators*, 3rd ed.; CRC Press: Boca Raton, FL, USA, 2015.
23. Krishna, V.B.M.; Sandeep, V.; Murthy, S.S.; Yadlapati, K. Experimental investigation on performance comparison of self excited induction generator and permanent magnet synchronous generator for small scale renewable energy applications. *Renew. Energy* **2022**, *195*, 431–441. [CrossRef]